Electronic Supplementary Material (ESI) for Soft Matter.
This journal is © The Royal Society of Chemistry 2016

Supplementary Material: Particle diffusion in active fluids is non-monotonic in size

Alison E. Patteson[1], Arvind Gopinath[1,2], Prashant K. Purohit[1] and Paulo E. Arratia[1]
[1] *Department of Mechanical Engineering & Applied Mechanics, University of Pennsylvania, Philadelphia, PA 19104.*
[2] *School of Engineering, University of California Merced, Merced, CA.*

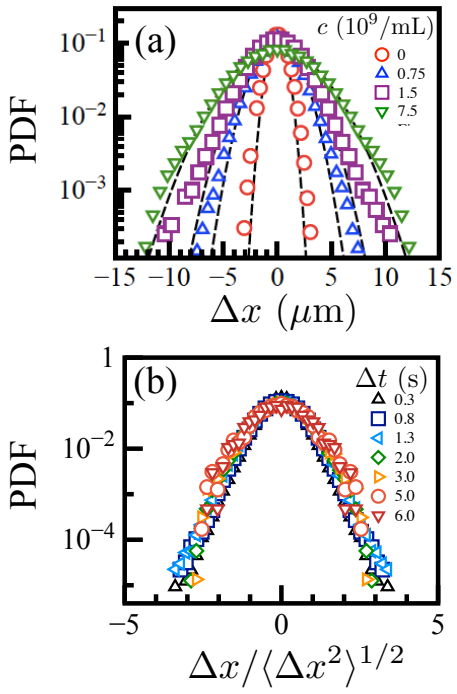

FIG. 1. (a) The probability distribution of 2 μm particle displacements PDF($\Delta x, \Delta t, c$) at $\Delta t = 2$ s for varying bacterial concentrations c. Dashed lines are fits to a Gaussian. (b) The collapse of the probability distribution at different time steps in a bacterial suspension with concentration $c = 7.5 \times 10^9$ cells/mL.

I. ROLE OF CONFINEMENT AND INTERFACIAL EFFECTS

The thickness of the film, h_f, is about 100 ± 20 microns with the particle diameter d ranging from $0.6 - 39$ μm. Thus the ratio $h_f/d \sim 150 - 3$. Given that the ratio is large for all except the largest particle, we consider possible confinement effects for the largest 39 micron particles. An upper bound for the thermal diffusivity in the absence of bacteria can be obtained by assuming that the particle spans the film and diffuses in the plane of the film using the Saffman-Delbruck [1] estimate. According to this theory, the diffusivity of a sphere (diameter $d \sim h_f$) completely confined in a free-standing film with viscosity μ surrounded by air with viscosity μ_a is given approximately by

$$D_0^f \approx \frac{k_B T_0}{3\pi\mu d}\left(\frac{3}{4}\left[\ln(2\frac{\mu}{\mu_a}) - 0.5772\right]\right).$$

Note that the diffusion of even the largest sized particles we used (39 μm) is not as confined as the expression assumes since the particle does not span the width of the film. Furthermore we note that the diffusivity $D_0^f \sim d^{-1}$, a functionality similar to the free thermal diffusivity D_0. Plugging in values for the viscosities of film, μ and air μ_a, we find $D_0^f \approx 0.05$ μm^2/s for the 39 micron particle.

For the lowest bacterial concentration we used, the effective diffusivity of the particle is approximately 0.1 μm^2/s, still higher than D_0^f. At concentrations greater than 1.5×10^9 cells/mL, the effective diffusivity is an order of magnitude higher and the particle diffusion is dominated by activity and not by confinement.

Particles are only tracked while in the plane of focus. For small particles ($d < 3$ μm), the sedimentation velocities are low (< 0.3 μm/s) and the particles do not sediment significantly over the time scale of the experiment. The sedimentation velocity of the 39 μm polystyrene particle in water is ≈ 50 μm/s. Before taking data, we allow the 39 μm to settle near the bottom of the film. While the particle is close to the surface, there is still a film of liquid and hence the comments in the previous paragraph still apply - *i.e.*, the effective diffusion is still dominated by activity. Any draining of the fluid that results in the particle breaching the surface occurs over scales much larger than the experimental times.

Finally, we consider the possible deformation of the interface from the particle due to the weight of the particle by estimating maximum induced curvatures. The settling particle exerts a force $F_g = \frac{1}{6}\pi g \mu \Delta\rho d^3$ on the interface. Here, $\Delta\rho \approx 0.05 \times 10^3$ kg/m^3 and $g \approx 9.8$ m/s^2. This force acts on a surface with projected area of roughly $A = \pi d^2/4$. The pressure exerted, F_g/A, is less than the capillary pressure $4\sigma/d$ suggesting that any surface deformation occurs with curvatures smaller than the particle curvature. Specifically for the 39 micron particle, the ratio $(F_g d/4\sigma A)$ is less than 10^{-5}.

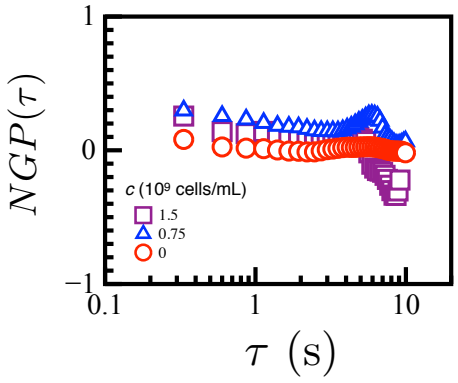

FIG. 2. The non-Gaussianity parameter of 2 μm particles over time τ in the absence ($c = 0$ cells/mL) and presence of E. coli ($c = 0.75$ and 3.0×10^9 cells/mL).

II. ROLE OF CONCENTRATION ON PARTICLE DYNAMICS

A. Collapse of particle distributions

To probe the effect of bacteria-particle interactions on long time particle displacements, we measure the van-Hove distribution - the probability distribution function (PDF) of particle displacements Δx - for varying concentrations of *E. coli* and different particle sizes. Shown in Fig. 1(a) are the PDF's of 2 μm particles measured over a fixed time interval $\Delta t = 2$ s. The PDF curves are nearly Gaussian (dashed lines are fits) indicating diffusive behavior with widths that increase as the concentration increases. When $c = 0$ cells/mL, the width of the distribution yields $D_0 \approx 0.2$ μm^2/s, consistent with the Stokes-Einstein prediction for a freely diffusing particle. In the presence of bacteria, while still approximately Gaussian, the PDF's exhibit deviations at the tail end, particularly a relative enhancement compared to the Gaussian fit. The tail-end deviations from Gaussianity tend to decrease at the highest bacterial concentration, $c = 7.5 \times 10^9$ cells/mL. These observations are consistent with previous experimental [2] and theoretical [3] studies of swimming microorganisms. These studies have shown that while the tail ends of particle displacement distribution function in the bulk [4] exhibit strong deviations from Gaussianity, the tail ends of the distribution function in a fluid film converge towards Gaussianity [2].

As shown in Fig. 1(b), we can collapse the PDF curves of particle displacements over time in the presence of *E. coli* ($c = 1.5 \times 10^9$ cells/mL), when the displacement Δx is rescaled by $\Delta x / \langle \sqrt{\Delta x} \rangle^2$.

The Gaussian nature of the particle distributions is further exemplified by the non-Gaussianity parameter NGP [5], which is defined as a function of time τ as

$$\mathrm{NGP}(\tau) = \frac{\langle \Delta x(\tau) \rangle^4}{3 \langle \Delta x(\tau)^2 \rangle^2} - 1,$$

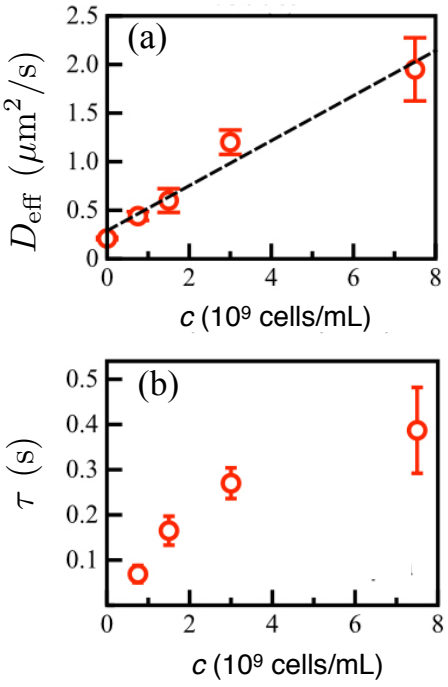

FIG. 3. (a) Effective diffusivities, D_{eff} for 2 μm particles, as a function of bacteria concentration, c. The trend is roughly linear, with a fitted slope (dashed line) consistent with previous results. (b) The corresponding crossover time τ increases monotonically with c.

where the brackets denote ensemble averages. For a Gaussian distribution, the NGP equals zero at all times, and thereby quantifies the deviation of a distribution from a Gaussian one over time. For the 2 μm particle distributions shown Fig. 1, we have calculated the NGP in the absence ($c = 0$ cells/mL) and presence of bacteria ($c = 0.75$ and 1.5×10^9 cells/mL), as shown in Fig. 2. As expected, in the absence of bacteria, when the system is in thermal equilibrium, the NGP is approximately zero (~ 0.1) at all times. For $c > 0$ cells/mL, the NGP values are still close to zero, which indicates that the distributions behave in a Gaussian way.

B. Effective diffusivity and cross-over time

We fit the MSD curves in Fig. 2(a) (main text) to the solution [6] for generic Langevin dynamics - eqn (1) in main text (see SI-§III for more details). This allows us to estimate D_{eff} and τ. When the particle size is held constant, both D_{eff} (Fig. 3(a)) and τ (Fig. 3(b)) increase with *E. coli* concentration.

For very dilute concentrations $\phi \ll 1$, particle-bacteria interactions are mainly binary [7] and we expect the enhancement in diffusivity to scale linearly with concentration. An alternate way to explain the linear dependence is to note that at low concentrations and in the absence of

collective motion or anomalous density fluctuations, fluctuations in bacterial concentration scale as $\sqrt{c}$ as given by the central limit theorem. The impulse due to these fluctuations sets the length scale characterizing bacteria-particle encounters; this length scale scales as $\sqrt{c}$ and thus the diffusivity scales as the square of this length $D_{\rm A} \sim {\rm O}(c)$. Indeed, our estimated values of $D_{\rm eff}$ increases linearly with bacterial concentration c, as shown by the dashed-line in Fig. 3(a). The variation of τ with concentration, however, does not follow a linear form. Instead, Fig. 3(b) suggests possible saturation of τ for suspensions of higher concentrations (but still dilute).

C. Comparison to previous experiments

The enhanced diffusion of passive particles in suspensions of swimming microorganisms has been previously verified in a variety of experimental techniques, including particle tracking methods in films [2], dye transport in microfluidic [8], and differential dynamic microscopy in three-dimensional chambers [9]. Previous investigators have proposed a linear relationship between the enhanced diffusivity and bacteria concentration to interpret their results [7, 9, 10] i,e., $D_{\rm eff} = D_0 + \beta U c$ where D_0 is the thermal diffusivity that follows the Stokes-Einstein relationship, U is the characteristic swimming speed (self-propulsive speed) of the microorganism and the quantity Uc has been called the active flux $J_{\rm A}$ [9, 10]. By dimensional arguments, it is clear that β has units (length)^4. Previous experimental investigations with *E. coli* have assumed β is constant and has a magnitude between 5 to 13 μm^4 [7–10]. A linear fit to Fig. 3(a) yields $\beta \approx 9$ μm^4 yields a reasonable fit consistent with the previous measurements mentioned above.

We also note discrepancies that support the contention that β is not really a constant, but varies with particle size. Following the theory by Kasyap. *et al.* [7], we rewrite $\beta = L^4 \bar{D}_A$, where L is the total length of the bacteria (7.6 μm for cell body and flagella) and $\bar{D}_A$ is a particle size-dependent dimensionless diffusivity which decays to zero at small particle diameter.

D. Spectral analysis

To quantify the velocity fluctuations, we measure the speed v of individual particles as a function of time, where the speed $v = \Delta\mathbf{r}/\Delta t$ is set by the frame rate $\Delta t = 1/30$ s. Next, a one-sided power spectra is then determined for each particle in a frequency range of 0.1 to 15 Hz, which corresponds to $2\Delta t$ to 10 s. The power spectra are normalized by $N/2$, where N is the number of data points. To determine an ensemble average within an experimental sample, we average the power spectra over individual particles, which have the same frequency binning intervals. As shown in Fig. 4, the power spectra are reasonably flat for varying *E. coli* concentrations and particle diameters. At equilibrium, the magnitude of the random thermal forcing, which appears as white noise, sets the temperature T [6], such that $\lim_{t\to\infty} \overline{v(t)v(t)} = \frac{k_B T}{m}$, where m is the mass of the particle. In the the infinite time limit, the initial conditions are forgotten.

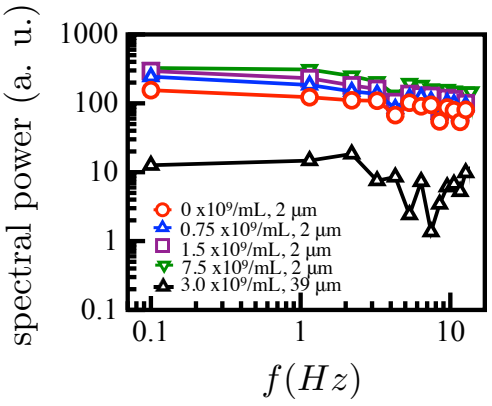

FIG. 4. Spectral density of particle speeds at varying *E. coli* concentrations of 0, 0.75, 1.5, and 7.5 $\times 10^9$ cells/mL and particle diameters of 2 μm and 39 μm.

Here, we find that the experimentally measured magnitudes of the power spectra increases with *E. coli* concentration for d =2 μm. As predicted by the infinite time limit, the increase in the magnitudes is consistent with an enhanced effective temperature (Fig. 5(a) main text). For $d = 39$ μm, the power spectra magnitude is reduced. This is expected since the increase in the variance of the particle speeds - i.e, the enhancement in the temperature is insufficient to overcome the increased mass.

III. MSD FOR A DIFFUSING PARTICLE

We consider a simple model of a spherical particle that undergoes an continuously diffusive process (due to both thermal and active effects) involving a sequence of small runs and random re-orientations. This is the case when the particle is buffeted around by interactions with bacteria. These assumptions are consistent with the sample trajectories shown in Fig. 5.

Let the particle be located at $\mathbf{r}(t)$ at time t and oriented with an angle $\theta(t)$. For ease of analysis, we let the particle move at a characteristic constant speed v between significant reorientations. The speed may be formally considered a function of the concentration of the bacteria and the particle size. The position and orientation of the particle follows $d\mathbf{r}/dt = v\mathbf{t}(t)$ and $d\theta/dt = \eta(t)$. Here, $\eta(t)$ is a zero-mean, delta-correlated Gaussian random variable such that $\langle \eta(t)\eta(t')\rangle = 2D_R\delta(t-t')$ and $\mathbf{t}$ is the instantaneous, local tangent to the trajectory. Note that here D_R is *not equal to* D_R^0, the rotational diffusivity in the absence of bacteria and purely due to Brownian ef-

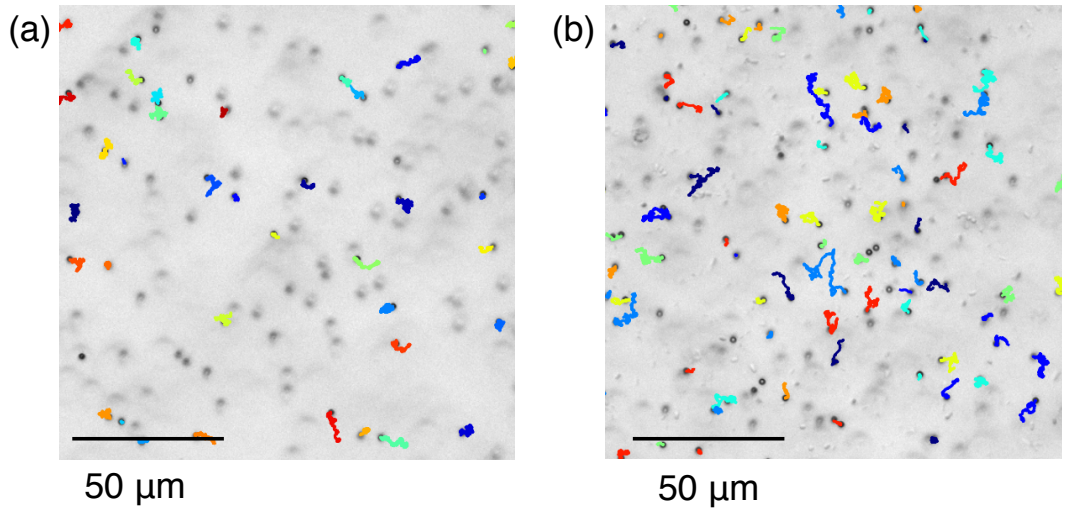

FIG. 5. Enhanced particle diffusion due to bacteria activity. Trajectories of 2 μm particles in a film of fluid (a) without and (b) with bacteria ($c = 0.75 \times 10^9$ cells/mL) reveal that particles in the presence of bacteria undergo larger magnitudes of displacement.

fects. Application of the central limit theorem shows that $\Delta\theta$ has zero mean and is distributed following a Gaussian profile. The pdf (probability density function), ψ is given by $\psi(t,\Delta\theta) = (1/4\pi t D_R)^{\frac{1}{2}} \exp(-\frac{\Delta\theta^2}{4\pi t D_R})$ which may then be readily used to calculate averages. The mean square displacement (MSD) is obtained by evaluation of the following integral expression $\langle|\mathbf{r}(t+\Delta t) - \mathbf{r}(t)|^2\rangle = v^2 \int_t^{t+\Delta t} dt' \int_t^{t+\Delta t} \langle\cos[\theta(t') - \theta(t'')]\rangle \, dt''$ and is found to be $\mathrm{MSD}(\Delta t) = 2\left(v^2/D_R\right)\left(t - \frac{1-e^{-\Delta t D_R}}{D_R}\right)$.

The effective translational diffusivity is obtained by now rewriting this expression. First, we introduce an average run time $\tau \equiv D_R^{-1}$, that characterizes the time for the MSD to transition from ballistic to diffusive behavior and is related to the time for the particle to forget its initial orientation. We then introduce an effective diffusivity D_{eff} that is the sum of its value at zero concentration and an excess concentration dependent *active* diffusivity $D_{\mathrm{eff}} = D_0 + D_A(c)$. To leading order for small concentration D_A is linear in bacterial concentration c when no collective motion exists. Adjusted for the two dimensional nature of the motion, the MSD then writes as

$$\mathrm{MSD}(\Delta t) = 4\left(D_0 + D_A\right)\Delta t\left(1 - \frac{\tau}{\Delta t}\left(1 - e^{-\frac{\Delta t}{\tau}}\right)\right). \tag{1}$$

Treating τ as a function of concentration, we take the limit of $c \to 0$ to obtain the formal solution in the limit of zero concentration $\mathrm{MSD}(\Delta t)(c=0) = 4D_0\Delta t\left(1 - \frac{\tau_0}{\Delta t}\left(1 - e^{-\Delta t/\tau_0}\right)\right)$ where $\tau_0 = \tau(c=0)$. Eqn (1) is valid in both active and passive limits and has indeed be used to investigate diffusion of particles in active fluids and biofilms [2, 11]. The long lag time limit taken when $\Delta t/\tau \gg 1$, gives us the asymptotic expression $\mathrm{MSD}(\Delta t \gg \tau) \sim 4\left(D_0 + D_A\right)\Delta t - 4\left(D_0 + D_A\right)\tau$ with corrections that are exponentially small. In the short lag time limit as $\Delta t/\tau \ll 1$ we find the asymptotic expansion $\mathrm{MSD}(\Delta t \ll \tau) \sim 2\left(D_{\mathrm{eff}}\right)(\Delta t)^2/\tau$.

An alternate analytical expression for the MSD has been derived previously and used to interpret the diffusion of active photo-colloids [12–14]:

$$\mathrm{MSD}(\Delta t) = 4\left(D_0 + D_A\right)\Delta t - 4D_A\tau\left(1 - e^{-\Delta t/\tau}\right). \tag{2}$$

Comparison of eqn (2) with eqn (1) reveals the following features. First the long time effective diffusivities D_{eff} predicted by the two expressions in the limit $\Delta t/\tau \to \infty$ are the same. Since $D_{\mathrm{A}} = D_{\mathrm{eff}} - D_0$ and D_0 is defined (and not a fitting parameter), the values of the active diffusivity obtained from both forms are the same. The short time asymptote of (1) and (2) for small lag time are however different. Equation (2) yields MSD $\sim 4\left(D_0 + D_A\right)\Delta t - 4D_A\tau\Delta t/\tau \sim 4D_0\Delta t$ in contrast to the superdiffusive (ballistic to leading order) asymptotic form from eqn (1). Furthermore in the limit of zero bacterial concentration when $D_A = 0$, eqn (2) does not reduce to the formal solution to the Langevin equation.

We have used both eqn (1) and (2) to fit our data. Since D_0 is not a fitting parameter but is given by the analytical Stokes-Einstein relationship, we fit for D_A and τ. We find that eqn (1) gives a better fit for τ for the two smallest particle sizes at small times. For other cases, both equations yield comparable values of τ. The values of D_A obtained from the long time asymptotes are the same for (1) and (2). Because of these considerations, we have chosen to use the MSD expression given by eqn (1) to analyze our data.

IV. PREVIOUS THEORY FOR SMALL AND LARGE PECLET NUMBER

Kasyap, Koch and Wu [7] recently presented a analytical theory supplemented by simulations of the diffusion of passive, Brownian particles in three dimensional suspensions of *E. coli* bacteria. They present an explicit expression for the hydrodynamic particle diffusivity $\overline{D}_{\rm A}$ resulting from bacteria-particle interactions. Their analytical theory assumes that encounters are binary, ignores steric interactions (which were however considered in more detailed simulations) and uses two additional simplifications - first that orientations of bacterium before and after a tumble are uncorrelated and second, that the fluid velocity disturbance created by each bacterium is small compared to its swimming speed, U.

Both the analytical theory and the simulations show that the scaled hydrodynamic diffusivity, $\overline{D}_{\rm A} = (D_{\rm eff} - D_0)/cL^4U$ is controlled by the two dimensionless parameters - the Peclet number, ${\rm Pe} \equiv UL/D_0$ (the ratio of the time scale of bacterial swimming to the particle diffusion time and $\tau_* \equiv U\omega_T^{-1}/L$, (the inverse of the tumble frequency ω_T to the time a bacterium takes to swim a distance equal to its length L). In all our experiments, we use the same strain of bacteria; thus, τ^* is held fixed. The theory predicts that $\overline{D}_{\rm A}$ is a monotonically increasing function of τ_* but a non-monotonic function of Pe. Below, we briefly summarize the theoretical predictions for small Pe$\ll 1$ and large Pe$\gg 1$.

Provided $\tau_* \geq O(1)$, as in our experiments, theory suggests that $\overline{D}_A \sim \sqrt{\rm Pe}$ for ${\rm Pe} \ll 1$. Thus the active diffusivity $D_A \sim cUL^4(UL/D_0)^{\frac{1}{2}}$; in terms of particle size d, this predicts $D_A \sim \sqrt{d}$. We do not access this small Peclet number regime in our experiments.

The asymptotic result for very large values of $\tau_* \gg 1$ with ${\rm Pe} \gg 1$ corresponds to non-Brownian particles in a suspension of non-tumbling bacteria. Both their analytical theory and simulations predict the enhancement in diffusivity to asymptote to constant values that are independent of the Peclet numbers as well as τ^*. For finite values of τ^* the value of $\overline{D}_A$ as ${\rm Pe} \to \infty$ depends only on τ^* and follows $\overline{D}_A \approx \frac{\alpha^2}{192\pi M^2} f(\tau_*)$, where α and M are bacteria related geometry parameters and $f(\tau_*)$ is a scalar function and controls the time scale over which the velocity disturbances induced by swimming bacteria stay correlated. The cells we use are wild type (strain MG1655) with run times of roughly 1 second and $\tau_* = 1.8$. From Fig. 5(b) in the main manuscript, we find that for the largest Peclet number we attain, $\overline{D}_A \approx 3.0 \times 10^{-3}$. This is consistent with asymptotic limits of $\overline{D}_A \approx 3.4 \times 10^{-3}$ and 4.2×10^{-3} for $\alpha = 2/7$ [15] and $M = 0.18$ at $\tau_* = 1$ and 4, respectively [7].

V. QUALITATIVE ESTIMATE FOR THE MAXIMUM EFFECTIVE PARTICLE DIFFUSIVITY $D_{\rm eff}$

Our experimental data suggests that both the existence and location of the peak can be tuned by adjusting c and d as independent parameters. We now consider a minimal model that yields a quantitative prediction for the existence as well as the location of the peak in $D_{\rm eff}$.

We first rewrite $D_{\rm eff}$ to explicitly incorporate its linear dependence on c:

$$D_{\rm eff} = D_0 + (cL^3UL)\overline{D}_A. \tag{3}$$

Differentiating $D_{\rm eff}$ with respect to Pe yelds

$$D'_{\rm eff} = (UL)\left[-\frac{1}{{\rm Pe}^2} + (cL^3)\overline{D}'_A\right]. \tag{4}$$

where primes denote differentiation. Setting eqn (4) to zero, we conclude that a extremum (shown to be a maximum from the data) in $D_{\rm eff}$ exists for

$$cL^3 = ({\rm Pe}^2\overline{D}'_A)^{-1}. \tag{5}$$

The collapsed universal curve (Fig. 5(b) in the main manuscript) depends on both Pe and τ^*; in our case τ^* is a constant. Using the experimentally collapse curve, we approximate the slope $\overline{D}'_A$ by fitting our data (Fig. 5(b)) to the form

$$\overline{D}_A({\rm Pe}) \approx \left[A_0 - \frac{1}{2}A_1({\rm Pe_A} - {\rm Pe})^2\right]. \tag{6}$$

Here $A_0 = \overline{D}_A({\rm Pe_A})$ with ${\rm Pe_A}$ being the Péclet number at which $\overline{D}_A$ is a maximum. In the general case, A_0, A_1 and ${\rm Pe_A}$ would be functions of τ^*. We fit the collapsed $\overline{D}_A$ data (Fig. 5(b)) for the range $200 < {\rm Pe} < 4000$ to eqn (6) and obtain ${\rm Pe_A} \approx 1000$ and $A_1 \approx 5 \times 10^{-7}$. From eqn (6), it follows that the slope is given by $\overline{D}'_A({\rm Pe}) \approx A_1({\rm Pe_A} - {\rm Pe})$. Note that eqn (6) is the simplest analytical form that allows us to model the variation in the vicinity of the maximum. Of course, far from the maximum, such a simple approximation will not be valid anymore and higher order terms will be required.

We next estimate the magnitude and location of the maximum $D_{\rm eff}$ by substituting eqn (6) into eqn (5). The Péclet number ${\rm Pe_{max}}$ at which $D_{\rm eff}$ is maximum is given by the cubic equation

$$cL^3A_1({\rm Pe_A} - {\rm Pe_{max}}) = {\rm Pe_{max}}^{-2}. \tag{7}$$

We are interested in how ${\rm Pe_{max}}$ changes with c and so we seek an approximate asymptotic real and physically valid solution for ${\rm Pe_{max}}$.

Let $\delta{\rm Pe}$ be a measure of the deviation from ${\rm Pe_A}$ defined through ${\rm Pe_{max}} = {\rm Pe_A} - \delta{\rm Pe}$. Note that ${\rm Pe_{max}} < {\rm Pe_A}$ so that by definition $\delta{\rm Pe} > 0$. We substitute ${\rm Pe_{max}} =$

$\mathrm{Pe_A} - \delta\mathrm{Pe}$ into eqn (7), Taylor expand the right and left hand sides, simplify the resulting expansions by utilizing the conditions ${\mathrm{Pe}_{\max}}^2 \gg 1$ and $\delta\mathrm{Pe} \ll \mathrm{Pe_A}$ and finally retain terms to $\mathrm{O}(\delta\mathrm{Pe})$. This then gives us the equation

$$\left(\mathrm{Pe_A^3} cL^3 A_1 - 2\right)\ \delta\mathrm{Pe} \approx \mathrm{Pe_A}. \tag{8}$$

The constraint that $\delta\mathrm{Pe} > 0$ results in the inequality $\mathrm{Pe_A^3} cL^3 A_1 > 2$ for a valid solution to exist. Furthermore, eqn (8) provides the shift in the peak, $\delta\mathrm{Pe}$ relative to $\mathrm{Pe_A}$, when it exists. Using the expression for $\delta\mathrm{Pe}$ from eqn (8) we obtain expressions for the location of the peak $\mathrm{Pe}_{\max}$ and thereby its dependence on c, $\mathrm{Pe}_{\max} = \mathrm{Pe_A}\left[1 - \left(\frac{1}{\mathrm{Pe_A^3} cL^3 A_1 - 2}\right)\right]$, and $d_{\mathrm{eff}}^{\max} = d_{\mathrm{A}}\left[1 - \left(\frac{1}{\mathrm{Pe_A^3} cL^3 A_1 - 2}\right)\right]$ is the corresponding location in particle size $d_{\mathrm{eff}}^{\max}$ where d_{A} is the particle diameter corresponding to $\mathrm{Pe_A}$. In our case, plugging in $A_1 \approx 5 \times 10^{-7}$ and $\mathrm{Pe_A} \approx 1000$, yields

$$d_{\mathrm{eff}}^{\max} = d_{\mathrm{A}}\left[1 - \left(\frac{1}{5cL^3 - 2}\right)\right] \tag{9}$$

Note that as c increases, $d_{\mathrm{eff}}^{\max}$ increases, consistent with our experimental observations (Fig. 3(a)).

The magnitude of the maximum effective diffusivity $D_{\mathrm{eff}}^{\max}$ is thus evaluated as $\frac{D_{\mathrm{eff}}^{\max}}{UL} = \frac{1}{\mathrm{Pe_A}} + cL^3\left(A_0 - \frac{A_1}{A_2}\right)$ where $A_2 = \frac{2}{\mathrm{Pe_A^2}}\left(\mathrm{Pe_A^3} cL^3 A_1 - 2\right)^2$.

VI. SUPPLEMENTARY VIDEOS

A. Movie 1

This video is of 2 micron particles at equilibrium, in the absence of bacteria. The video is played at real time.

B. Movie 2

This video is of 2 micron particles in the presence of *E. coli* at bacterial concentration $c = 1.5 \times 10^9$ cells/mL. The video is played at real time.

C. Movie 3

This video is of a 39 micron particle in the presence of *E. coli* at bacterial concentration ($c = 1.5 \times 10^9$ cells/mL). The video is played at real time.

D. Movie 4

This video is of a 39 micron particle in the presence of *E. coli* at bacterial concentration ($c = 7.5 \times 10^9$ cells/mL). The video is played at real time. Even at the highest bacterial concentration, there is no large-scale collective behavior of the bacteria in the bulk.

[1] P. G. Saffman and M. Delbruck, Proc. Natl. Acad. Sci., **72** 3111-3113 (1975).
[2] H. Kurtuldu, J. S. Guasto, K. A. Johnson and J. P. Gollub, Proc. Nat. Acad. Sci., **108**, 10391 (2011).
[3] I. M. Zaid, J. Dunkel, and J. M. Yeomans, J. R. Soc. Interface, **8**, 1314-1331 (2011).
[4] K. C. Leptos, J. S. Guasto, J. P. Gollub, A. I. Pesci and R. E. Goldstein, Phys. Rev. Lett., **103**, 198103 (2009).
[5] T. Toyota, D. A. Head, C. F. Schmidt, and D. Mizuno, Soft Matter, **7**, 3234 (2011).
[6] R.K. Pathria, *Statistical Mechanics*, (Butterworth, Oxford, 1996).
[7] T. V. Kasyap, D. L. Koch, and M. Wu, Phys. Fluids, **26**, 081901 (2014).
[8] M. J. Kim and K. S. Breuer, Phys. Fluids, **16**, L78 (2004).
[9] A. Jepson, V. A. Martinez, J. Schwarz-Linek, A. Morozov, and W. C. Poon, Phys. Rev. E, **88**, 041002 (2013).
[10] G. Mino, T. E. Mallouk, T. Darnige, M. Hoyos, J. Dauchet, J. Dunstan, R. Soto, Y. Wang, A. Rousselet, and E. Clement, Phys. Rev. Lett., **106**, 048102 (2011).
[11] L. Vaccari, D. B. Allan, N. Sharifi-Mood, A. R. Singh, R. L. Leheny and K. J. Stebe, Soft Matter, **11**, 6062-6074 (2015).
[12] J. Palacci, C. Cottin-Bizonne, C. Ybert and L. Bocquet, Phys. Rev. Lett., **105**, 088304 (2010).
[13] N. Koumakis, C. Maggi, and R. Di Leonardo, Soft Matter., **10**, 5695 (2014).
[14] C. Maggi and M. Paoluzzi, N. Pellicciotta, A. Lepore, L. Angelani and R. Di Leonardo, Phys. Rev. Lett., **113**, 238303 (2014).
[15] H. Berg and L. Turner, PNAS, **92**, 477-479 (1995).